JOURNAL OF PROPULSION AND POWER
Vol. 24, No. 1, January–February 2008

Effect of High-Voltage Pulsed Discharges on Deflagration to Detonation Transition

V. P. Zhukov,* A. E. Rakitin,† and A. Yu. Starikovskii‡
Moscow Institute of Physics and Technology, 141700, Dolgoprudny, Russia

DOI: 10.2514/1.29442

An experimental study of ignition and detonation initiation by two different kinds of high-voltage pulsed gas discharge has been performed in two smooth detonation tubes. The experiments were carried out at pressures ranging from 0.15 to 1 bar in various gaseous stoichiometric mixtures. In the first setup, a distributed nonequilibrium nanosecond discharge was used for mixture excitation and ignition. In the second setup, a localized microsecond pulsed spark discharge with a stored energy of 14 J developed. The electrical parameters of the discharges, ignition delay time, flame front, and shock wave velocities were measured in the experiments. Essentially, higher efficiency of the nanosecond discharge as a detonation initiator has been demonstrated: deflagration to detonation transition was observed 3 tube diameters away from the discharge chamber in different $C_3H_8/C_4H_{10} + 5O_2 + xN_2$ and $0.5C_6H_{14} + 4.5O_2 + xN_2$ mixtures with N_2 concentrations up to 38%. The energy input in these cases did not exceed 3 J, and the deflagration to detonation transition time was less than 1 ms. The microsecond spark discharge ignited the mixture efficiently, but the transition length and time increased significantly.

I. Introduction

CONTEMPORARY research in the field of gaseous detonations is closely related to the realization of the pulsed detonation engine (PDE) concept. A fuel–oxidizer mixture combustion in a PDE is a decreasing-volume process which occurs at higher pressures and temperatures as compared to the conventional constant-pressure combustion and allows one to achieve significantly higher thermodynamical efficiency. A detonation wave may be formed by a direct initiation or through a deflagration-to-detonation transition (DDT) process. For a direct detonation initiation, an ignition source of a considerable energy is required. In a stoichiometric propane–air mixture, ignition may be obtained with a spark discharge with an energy of 1 mJ, whereas for a direct initiation of a spherical detonation in the same mixture a minimum energy of 0.08 kg in trinitrotoluene (TNT) equivalent or 300 kJ is required [1]. When initiated by a lower energy source in a sufficiently long tube, a DDT may occur through the flame front acceleration. In this case, the typical DDT length amounts to several tens of tube diameters. Thus, because DDT length and time are crucial parameters for PDE applications, one of the key issues is the reduction of the transition length and time in detonation tubes under a minimum energy of initiation.

A number of means for DDT facilitation is well known. The most common method of DDT length reduction is the application of various types of obstacles which disturb the flow and increase the flame velocity. This method has been proposed by Shchelkin [2], who used wire spirals inside the tube for flow turbulization, and has been since widely applied in a number of works [3–7]. A modification of this method is the application of a two-chamber initiating system [8,9]. In this case, a smaller auxiliary chamber is used for primary ignition by a weak ignition source, whereas the mixture in the main chamber is ignited by flame jets coming out of the auxiliary chamber. Detonation initiation by shock wave focusing with shaped reflectors (experimental [10,11]) and with regularly spaced shaped obstacles (numerical [12]) was also proven possible. In the latter work, the focusing effect of shaped obstacles upon shock-to-detonation transition was emphasized: in the case with rectangular shaped obstacles no focusing occurred and detonation was not observed under identical conditions. Another possible way to promote a DDT process is the gradient mechanism theoretically proposed by Zeldovich [13] and numerically modeled in a number of works [14–16]. A similar idea of coupling the energy release with the amplification of the leading shock wave was also introduced in shock wave amplification by a coherent energy release (SWACER) mechanism [17]. A coherent ignition technique similar to the SWACER mechanism was used experimentally for detonation wave formation in [18]. In the experiments, the mixture was ignited by a set of properly synchronized spark plugs installed along the detonation tube, which resulted in significant reduction of the DDT length and of the initiation energy for the case. A number of research groups carried out experimental investigations of ignition and detonation initiation by nonequilibrium pulsed corona discharges [19]. The experiments confirmed that ignition delay times decreased substantially in comparison to spark initiation.

Pulsed discharge in the form of a fast ionization wave (FIW) was proposed as a tool for DDT length and time reduction in [20]. In this paper, the nonequilibrium plasma of a high-voltage (HV) nanosecond gas discharge was used for simultaneous preexcitation of the gas and for the reduction of ignition delay time in a bulk volume. The calculations performed for hydrogen–air and methane–air mixtures showed that the ignition threshold shifted by 400 K under an energy deposition of 0.4 J/cm^3 in the methane–air mixture. It was also shown that the typical time of chemical energy release had to be shorter than that of the gas-dynamic processes to form a detonation wave. Thus, for DDT length reduction it is desirable that the sonic speed and, hence, the temperature be as low as possible, which is the case in a nonequilibrium plasma of a high-voltage nanosecond gas discharge.

It is important that this kind of discharge developed in a chamber of a proper geometry is capable of instantly ionizing and exciting the gas in a bulk volume. This may lead to simultaneous mixture ignition over that volume resulting in volumetric explosion and, possibly, in a direct initiation of detonation. On the other hand, in terms of Zeldovich's gradient mechanism of DDT promotion, an ignition delay time gradient may be formed by a radical concentration gradient, which may be in turn produced by the discharge. Because of the spatial homogeneity of this kind of discharge, it is possible to form the gradient in a large volume rather than only in the close vicinity of hot spots. Thus, the nanosecond discharge is very

Received 25 December 2006; revision received 10 September 2007; accepted for publication 4 October 2007.

*Research Scientist, Physics of Nonequilibrium Systems Laboratory.
†Ph.D. Student, Physics of Nonequilibrium Systems Laboratory.
‡Associate Professor, Head of Research Center, Physics of Nonequilibrium Systems Laboratory.

promising for detonation initiation and DDT facilitation from a number of points of view. To realize the advantages of this initiation method, a proper geometry and parameters of the discharge chamber are required.

Relying on these results, Zhukov and Starikovskii carried out experiments on detonation initiation by this kind of discharge [21–23]. A 131-cell discharge chamber with a distributed electrode system was developed and patented [24]. A study of the discharge development with an intensified charge-coupled device (ICCD) camera showed that the discharge was distributed over the cross section of the chamber, filling a significant portion of the cells. This was achieved due to the short rise time and width of the high-voltage nanosecond pulse. The experiments were carried out in propane–oxygen and propane/butane–oxygen mixtures diluted with nitrogen at initial pressures from 0.15 to 0.55 bar. It allowed one to achieve a DDT length of 130 mm in a smooth tube in a $C_3H_8 + 5O_2$ mixture at 0.3 bar of initial pressure and 70 mJ of discharge energy. Discharge development and detonation wave formation were studied with a fast ICCD camera, pressure transducers, and infrared (IR) sensors. It was found that the efficiency of the distributed nanosecond detonation initiation strongly depended on the nitrogen dilution level and initial mixture pressure, whereas the dependence upon the discharge energy was weak.

The aim of the current work is to extend the research discussed in [21] and to study the effects of different discharge types upon DDT in smooth tubes. For that, experiments on detonation initiation by high-voltage microsecond discharge have been carried out and the results have been compared to those obtained for nanosecond discharge initiation. The study of the latter has been extended up to higher pressures, which allows one to make the comparison in a wider range of initial parameters. The results presented have been partially published at various AIAA conferences. The current paper summarizes all of them, as well as those presented in [21], proposing mechanisms responsible for detonation initiation by high-voltage pulsed discharges.

II. Detonation Initiation by Nanosecond Discharge at Pressures up to 1 Bar

The experimental setup used for the study of detonation initiation by the distributed high-voltage nanosecond discharge and the experimental parameters were discussed in [21]. The detonation tube had an inner diameter of 140 mm; the multicell discharge section mounted at one end of the detonation tube was a distributed electrode system consisting of 131 discharge cells placed over the cross section of the tube. Each discharge cell included a pinlike high-voltage electrode inside a quartz tube covered from the outside with a grounded foil (see Fig. 1). The foil was grounded through an aluminum orificed plate at the output end of the discharge chamber. The orificed plate was adjusted so that the conical orifices coincided with the discharge cell outputs. The cone angle was 30 deg, which ensured flow attachment to the cone walls. The diameters of all the discharge cells and orifices were 5 mm, and the interelectrode gap was 80 mm. The high-voltage electrodes of the distributed electrode system were fed with high-voltage nanosecond pulses with a rise time of 15 ns and a width of 50 ns, the amplitude being varied from 4 to 70 kV. In addition to the previously used five IR detectors, two schlieren sensors had also been installed 37 and 287 mm away from the discharge chamber, which corresponded to the positions of the first and the third IR detectors. Each sensor included a laser, a triangular reflecting prism, and two photodiodes connected to a differential amplifier which would yield zero if no density disturbance occurred. A nonzero amplifier signal corresponded to a density gradient passing through the laser optical path, thus deflecting the laser beam and unbalancing the scheme. The schlieren sensors allowed us to measure compression wave velocity along with the flame propagation velocity measured by the IR detectors.

The experiments in detonation initiation in the higher pressure region were carried out in stoichiometric mixtures of two fuels: $C_3H_8/C_4H_{10} + 5O_2 + xN_2$ ($0 \le x \le 10$) and $0.5C_6H_{14} + 4.5O_2 + xN_2$ ($0 \le x \le 3$). Initial pressure values were varied from 0.2 to

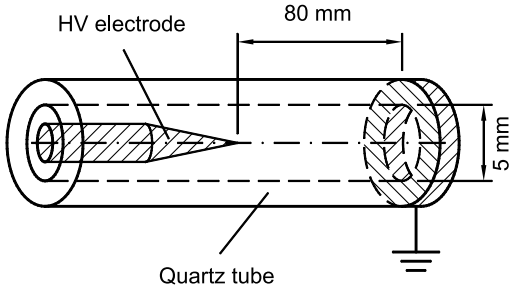

Fig. 1 One of the 131 cells of the multicell discharge chamber [24].

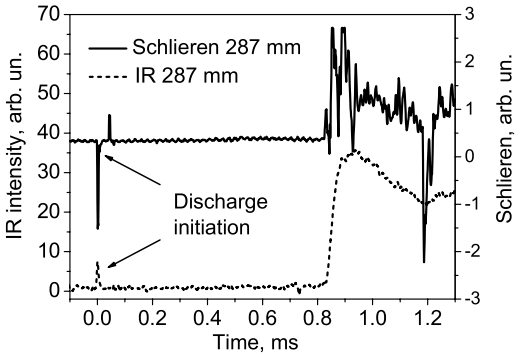

Fig. 2 Schlieren sensor and IR sensor signals 287 mm away from the discharge chamber.

1 bar. In the experiments, flame front velocity, compression/shock wave velocity, and ignition delay times were measured simultaneously with initial mixture pressure, nitrogen dilution level, and nanosecond pulse parameters. The comparison of the results obtained with the IR detectors and the schlieren sensors showed that flame front velocity was equal to shock wave velocity in all supersonic propagation modes. See Fig. 2 for the schlieren sensor and the IR detector signals 287 mm away from the discharge chamber; the figure corresponds to a C–J detonation propagating in a $0.5C_6H_{14} + 4.5O_2 + 3N_2$ mixture at 0.76 bar of initial pressure. This proved the possibility to use IR emission diagnostics for DDT study. This would also allow us to compare the velocity values obtained with the IR detectors with those obtained with the pressure transducers in the supersonic modes.

The results of the experiments are presented in Fig. 3 in terms of dependencies of the flame front propagation velocity 400 mm ($\sim$3 tube diameters) away from the discharge chamber upon initial mixture pressure for different mixture compositions. The corresponding results for lower pressures from [21] are also presented in the same figure for comparison. It is seen from the figure that the flame front velocities in propane/butane and hexane mixtures are almost the same for the mixtures with close nitrogen dilution values, for which the combustion heat values are also close. Velocity values of $\sim$2400 m/s for the propane/butane mixtures (hollow symbols and solid lines) and $\sim$2100 m/s for the hexane mixtures (solid symbols and dashed lines) correspond to the experiments where C–J detonation was observed. Successful DDT was observed 3 tube diameters away from the discharge chamber or closer in all mixtures with a nitrogen dilution level up to 38% under initial pressures up to 1 bar. In all these cases the DDT time was below 1 ms under initiation energy under 3 J.

III. Detonation Initiation by Microsecond Spark Discharge

A. Experimental Setup

To compare detonation initiation and flame propagation modes under different initiation conditions, a new setup has been assembled. The setup scheme is presented in Fig. 4. The inner diameter and the length of the detonation tube (1) were 53 and

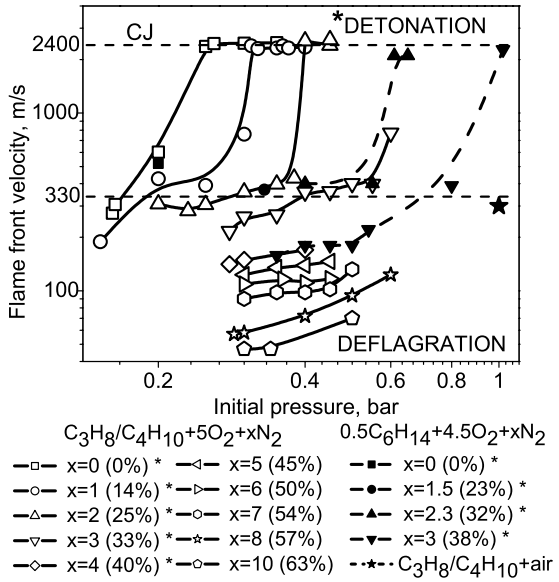

Fig. 3 Flame front velocity dependency upon initial mixture pressure for different mixture compositions under initiation by nanosecond discharge.

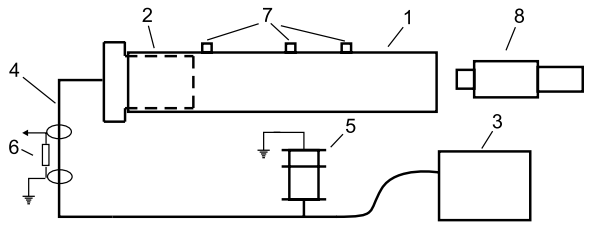

Fig. 4 Principal scheme of the setup with microsecond spark discharge: 1—detonation tube, 2—discharge chamber, 3—dc power supply, 4—feeding line, $Z = 17\ \Omega$, 5—thyratron, 6—backcurrent shunt, 7—pressure transducers, and 8—ICCD camera.

1000 mm, respectively. The discharge chamber (2) was mounted at the end of the tube. The geometry of the discharge chamber pictured in Fig. 5 was analogous to the one used for detonation initiation by the nanosecond discharge [21]. The high-voltage electrode was a distributed electrode system consisting of 28 pins separated from each other and from the ground electrodes by a ceramic insulator. Each pin formed a discharge cell with an interelectrode gap of 50 mm. The diameter of each cell was 5 mm; the cells were again connected with the detonation tube volume by conical nozzles with an angle of 30 deg. The dc power supply (3) charged the feeding line (4) up to a voltage of 37 kV. A high-voltage pulse was formed on the electrode after the feeding line had been grounded by the thyratron (5). The pulse parameters were registered by the backcurrent shunt (6).

The piezoelectric pressure transducers (7) were used for shock and detonation wave velocity measurements. The transducers were installed in the sidewalls of the tube at distances of 3, 363, and 873 mm from the discharge chamber. A typical oscillogram of the pressure transducer signals is presented in Fig. 6. In this case, the DDT took place between the first and the second transducers. The error in the pressure wave velocity measurement was mainly determined by the signal rise time. In the detonation mode, the error value was insignificant due to the steepness of the shock wave front, whereas, for deflagration modes, the error could reach $\sim$20 m/s.

The pulse amplitude was 37 kV, and the pulse width was 1–3 μs with $\sim$100 ns rise time. The rise time was determined by the thyratron switching time. The energy input in this case was limited by the energy stored in the feeding line, which was equal to 14 J. The actual energy input value was not measured in the experiments. The images of the discharge development were taken through the end

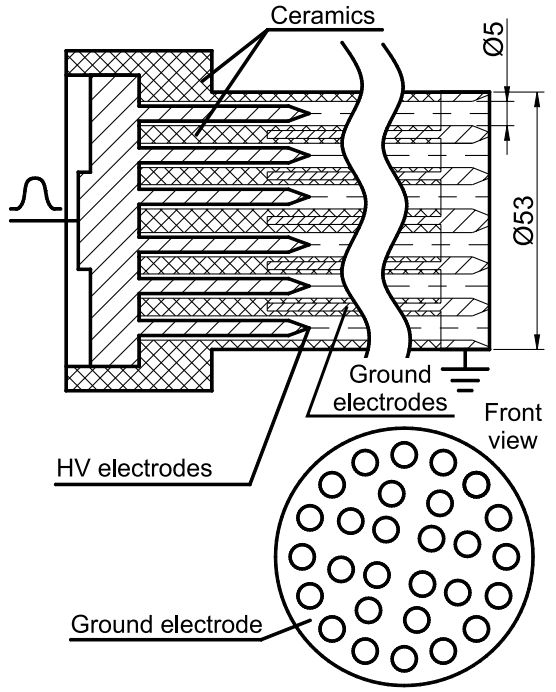

Fig. 5 Discharge chamber (2) consisting of 28 discharge cells: chamber diameter—53 mm, discharge cell diameter—5 mm, discharge cell length —95 mm, and interelectrode gap—50 mm [24].

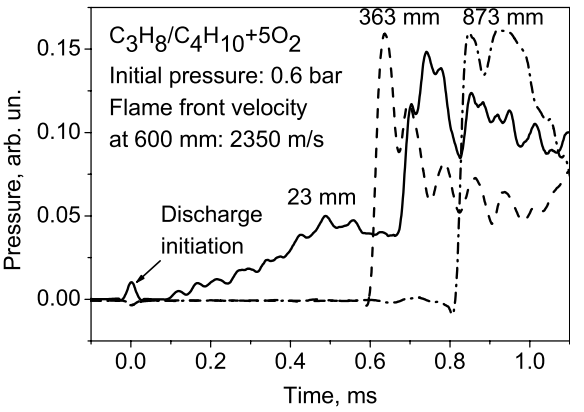

Fig. 6 Typical oscillogram of the pressure transducer signals.

plate of the detonation tube with a LaVision PicoStar HR12 ICCD camera (8) with nanosecond temporal resolution in the spectral range of 300–800 nm.

B. Microsecond Discharge Development

The microsecond discharge development was studied with the ICCD camera by the same technique which was used for the nanosecond discharge in [21]. Additionally, a temporal dependence of the integral discharge emission was registered with a photoelectric multiplier (PEM). These measurements allowed us to register the temporal dynamics of energy input in the discharge. The temporal dependence of the discharge emission in air at 1 bar is presented in Fig. 7 together with the backcurrent shunt signal. The corresponding spatially resolved negative ICCD images of the discharge are presented in Fig. 8. The black line in the image corresponds to the edge of the discharge chamber. The streamer phase of the discharge development at 1 bar is presented in Figs. 8a and 8b. The emission intensity at this stage was extremely low. The discharge localization and the spark formation due to ionization instability occurred sooner than $\sim$50 ns after the pulse had reached the electrode. The spark stage of the discharge development is presented in Figs. 8c and 8d. It

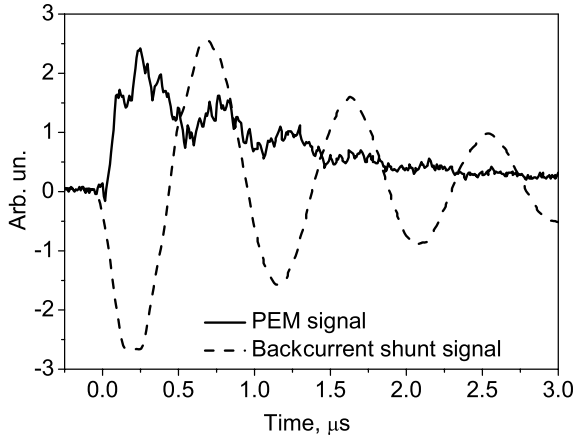

Fig. 7 PEM signal (solid line) and backcurrent shunt signal (dashed line).

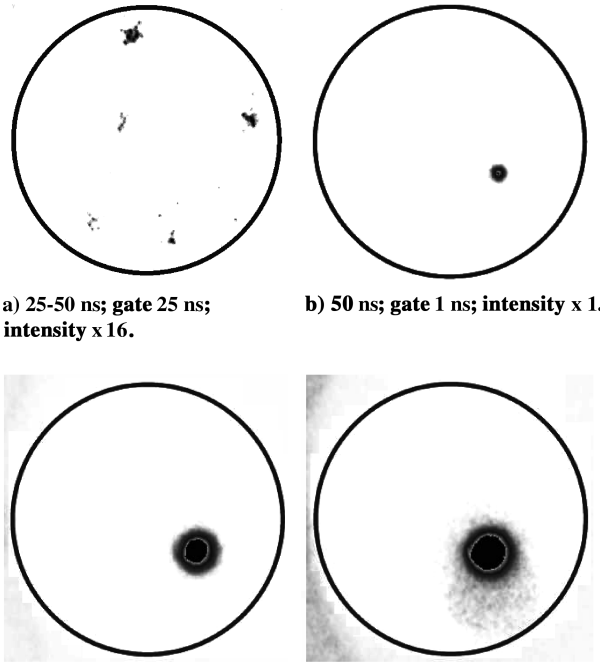

a) 25-50 ns; gate 25 ns; intensity x 16.

b) 50 ns; gate 1 ns; intensity x 1.

c) 65 ns; gate 1 ns; intensity x 1.

d) 230 ns; gate 1 ns; intensity x 1.

Fig. 8 Negative images of the microsecond discharge development.

was at these stages when most pulse energy consumption occurred. The distributed discharge phase was not observed at all in most discharge cells. Such a discharge development pattern is a result of a relatively long pulse rise time (~100 ns).

C. Ignition And Detonation Initiation by Microsecond Spark

The experiments on detonation initiation by the high-voltage microsecond discharge were carried out in two propane/butane mixtures ($C_3H_8/C_4H_{10} + 5O_2 + xN_2$ with $x = 0$ and $x = 4$) at initial pressures up to 1 bar. The mode of flame propagation was determined on the basis of the shock wave velocity measurements with the pressure transducers. As has been shown previously, the flame front velocity coincides with the shock wave velocity in all the supersonic modes. The results of these experiments are presented in Fig. 9 (solid lines, solid symbols) in terms of the dependencies of the shock wave velocity 600 mm (~11 tube diameters) away from the discharge chamber upon initial mixture pressure for different mixture compositions. The results are presented in comparison with those obtained in the same mixtures under initiation by the distributed nanosecond discharge (dashed lines and hollow symbols). It is worth

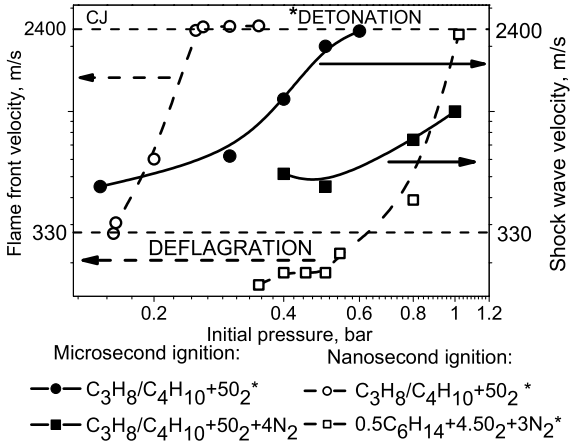

Fig. 9 Shock wave and flame front velocity dependencies upon initial mixture pressure for different mixture compositions. Solid lines and solid symbols stand for microsecond initiation; dashed lines and hollow symbols for nanosecond initiation.

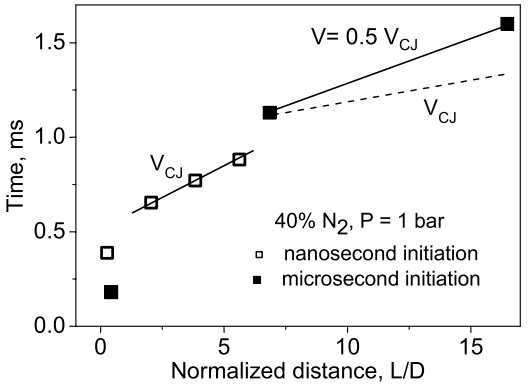

Fig. 10 *x–t* diagram for fuel–oxygen mixture with 40% N_2 under initiation by different kinds of discharge.

noting that these results are to be compared only in the region of supersonic propagation velocities. For the undiluted mixture (hollow circles), a C–J detonation was observed at $P = 0.6$ bar of initial pressure under initiation by the microsecond spark, whereas in the case of initiation by the nonequilibrium nanosecond discharge (solid circles) the DDT was obtained at an essentially lower pressure of 0.25 bar. For the mixture with a nitrogen dilution level of $x = 4$ (hollow squares), a C–J detonation was only observed under the nanosecond initiation. In the case of the microsecond spark initiation (solid squares), at the maximum initial pressure of 1 bar, a transient detonation mode with the flame front velocity of ~1000 m/s was observed. The higher efficiency of the distributed nanosecond discharge in terms of DDT run-up distance is illustrated by the *x–t* diagram in Fig. 10, which presents the *x–t* dependencies for the fuel–air mixture at 1 bar of initial pressure under different kinds of initiation. The diagram is plotted against normalized distance which is the ratio of distance in mm to the corresponding tube diameter. It is seen that under the nanosecond initiation the run-up distance is less than 2 tube diameters for the case, whereas under the microsecond initiation the velocity at 15 diameters is still significantly below the C–J value. The DDT time is also shorter for the nanosecond initiation. This indicates a significantly higher efficiency as a detonation initiator of the distributed nanosecond discharge when compared to the localized microsecond spark, at least in terms of DDT length and time under comparable energies of initiation.

Simultaneously in the same experiments mixture ignition was studied by measuring the ignition delay time dependency upon initial mixture pressure and nitrogen dilution level. The ignition delay time was determined from the delay between the discharge initiation and the onset of the signal of the first pressure transducer located 23 mm

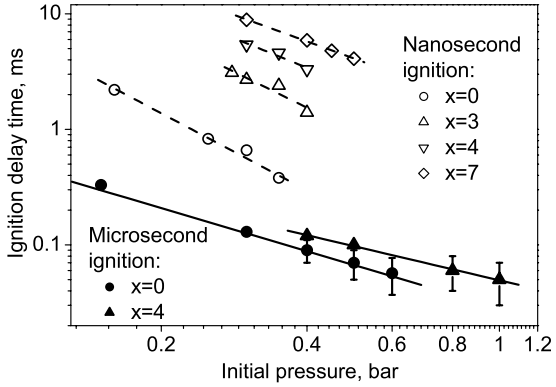

Fig. 11 Ignition delay time dependencies upon initial pressure. Mixtures: $C_3H_8/C_4H_{10} + 5O_2 + xN_2$.

away from the discharge chamber. The flame front propagation time from the discharge chamber to the pressure transducer was taken into account in these cases ($\sim$50 μs) because its value was comparable to the value of the typical ignition delay times. The ignition delay time dependence in various mixtures is presented in Fig. 11. The results for the ignition by the microsecond spark discharge are represented by solid symbols. The data for the hollow symbols correspond to the ignition by the distributed nanosecond discharge and were taken from [5]. It is seen that in the log–log scale the dependencies are straight lines, the slopes being different for different ignition types. It is noteworthy that the values of the ignition delay times are substantially lower for the microsecond ignition in all the mixtures at initial pressures up to $\sim$0.5 bar.

IV. Discussion

The experiments in detonation initiation by the high-voltage nanosecond discharge in the detonation tube with a 140-mm diameter showed that, as nitrogen dilution level increased (the mixtures with $x \geq 3$ in Fig. 3), the DDT at a distance of 400 mm from the discharge chamber occurred at increasingly higher initial pressures (0.4 bar and higher). In the stoichiometric propane/butane–oxygen mixture with N_2 dilution, the minimal initial pressure for the DDT to be observed increased from 0.3 to 0.4 bar when nitrogen concentration in the mixture was increased from 14 to 25%, whereas at a nitrogen concentration of 33% the minimal initial pressure amounted to 0.6 bar. When the dilution reached 38%, the DDT was only observed at an initial pressure of 1 bar. The dependence of the flame front velocity upon initial pressure in the region of nonstationary transient detonations became less steep: for the weakly diluted mixtures (with nitrogen concentrations below 33%), transient modes were observed in a $\sim$0.05 bar wide range of initial pressures, whereas in the mixture with 40% of nitrogen transient modes were observed at various initial pressures from 0.6 to 1 bar.

At the same time the typical flame front acceleration decreased substantially as the nitrogen concentration increased. In the $C_3H_8/C_4H_{10} + 5O_2 + N_2$ mixture, the acceleration reached $\sim 3 \times 10^6$ m/s at an initial pressure of 0.3 bar, whereas it amounted to only $\sim 4 \times 10^5$ m/s^2 in the $0.5C_6H_{14} + 4.5O_2 + 3N_2$ mixture at an initial pressure of 0.8 bar. Low values of the flame front acceleration lead to a longer transient mode and, thus, to the increase of the DDT length. This is also related to the less steep dependency of the flame front velocity upon initial pressure in transient modes. Because in a transient detonation mode the pressure wave is a shock wave propagating in front of the flame, the dependence of the flame front acceleration and velocity upon initial pressure is remarkably steeper in this mode than that in a deflagration.

To compare detonation initiation efficiency by the distributed nanosecond and the localized microsecond discharge, experiments were carried out in the detonation tube with the discharge chamber of analogous geometry. Both initiating devices consisted of a number of discharge cells of equal diameter distributed over the cross section with the same density. Each cell was connected to the main tube with a 30 deg conical nozzle. The tube diameters were different: 140 mm for the nanosecond initiation and 53 mm for the microsecond initiation. However, the comparison was made for the mixtures with detonation cell sizes substantially smaller than both tube diameters: the detonation cell size was 3.8 mm for the $C_3H_8 + 5O_2$ mixture at 0.25 bar, 4.0 mm for the $C_3H_8 + 5O_2 + 4N_2$ mixture at 1 bar, and 6.3 mm for the $0.5C_6H_{14} + 4.5O_2 + 3N_2$ mixture at 0.4 bar [25]. This allowed us to consider the conditions for DDT to be close for the two detonation tubes.

The results of the comparison presented in Fig. 9 indicate that detonation initiation efficiency in the setup with the nanosecond ignition is remarkably higher. The conditions of detonation initiation in the two setups differ mostly in the temporal and spatial shape of the discharge. The discharge chamber geometry difference itself influences the detonation initiation and propagation to a lesser extent. Nevertheless, the discharge chamber geometry together with the high-voltage pulse shape governs the discharge temporal and spatial shapes. The ICCD imaging with nanosecond temporal resolution showed that the discharge developed essentially differently in the two setups. It was shown in [21] that during the early stages ($t < 50$ ns) the nanosecond discharge is distributed over the cross section of the chamber filling a larger portion of the cells. The intensity falls sharply during the later stages. This indicates that most energy was deposited during the first 50 ns of the discharge development in agreement with the temporal shape of the electrical pulse. Under typical values of pressure (0.1–1 bar), voltage amplitude (10–70 kV), and rise time (>1 kV/ns), both gas ionization and dissociation occur during very short times over the volume of each discharge cell. The typical temporal scales of these processes are shorter than the typical gas-dynamic times. At the same time, a relatively low portion of energy is deposited into translational degrees of freedom. Instead, active radicals are produced in the discharge with their generation rate being governed by the reduced electric field value. Depending on the distribution of the active radicals along the cell, the mixture may be ignited almost simultaneously all over the cell producing a volumetric explosion or a combustion wave may emerge at the tip of the pinlike electrode. In the latter case the combustion wave may theoretically be intensified and accelerated by Zeldovich's gradient mechanism if a proper radical concentration gradient has been formed. Either way, the simultaneous exit of sufficiently intensive combustion or shock waves from a large number of discharge cells into the detonation tube may lead to a rapid formation of a detonation wave. An experimentally observed onset of detonation at a distance of less than one tube diameter at an initial pressure of 0.25 bar confirms high efficiency of detonation initiation by the distributed high-voltage nanosecond discharge.

In the setup with the microsecond ignition, the discharge development starts at the reduced electrical field values close to the breakdown value due to a long rise time of several hundreds of nanoseconds. Because high values of overvoltage cannot be reached, the breakdown develops in the form of a streamer discharge, which is transformed into a localized spark discharge within $\sim$1 μs in a single cell. In this case, a considerable portion of the energy is deposited into the heating of the gas and the formation of only one hot spot. This results in significantly shorter ignition delay times in comparison with the nanosecond ignition in the same mixtures (see Fig. 11). However, a rapid ignition in a single cell does not lead to an effective shock wave formation and acceleration in the main tube volume and, thus, is not an effective means for detonation initiation. On the other hand, the distributed nanosecond discharge generates a lot of ignition spots with a high density of radicals and a relatively low temperature. These spots need more time for developing, but the simultaneous ignition in numerous points results in a more successful deflagration to detonation transition.

V. Conclusions

The experimental study of detonation initiation by a high-voltage distributed nanosecond discharge has been extended into the region of higher initial pressures up to 1 bar. Under this kind of initiation a

successful DDT in a 140-mm diam smooth detonation tube was observed at 3 tube diameters from the discharge chamber in all the $C_3H_8/C_4H_{10} + 5O_2 + xN_2$ mixtures with N_2 concentrations up to 38%. The energy input did not exceed 3 J, and the DDT time was less than 1 ms.

Another setup has been assembled to experimentally study detonation initiation by high-voltage microsecond discharge. The images of the discharge development with nanosecond temporal resolution were taken by an ICCD camera. The microsecond discharge developed into a localized spark discharge within 50 ns at atmospheric pressure. Under this kind of initiation in a 53-mm diam smooth detonation tube, the DDT was observed at higher initial pressures for the same mixtures as compared to the distributed nanosecond initiation. Under equal initial conditions, the run-up distance in tube diameters for the initiation by the microsecond spark was significantly longer than that for the distributed nanosecond initiation. Thus, a higher efficiency of detonation initiation in terms of DDT length and time has been demonstrated by the nanosecond discharge as compared to the microsecond spark discharge. At the same time, the ignition delay times under the microsecond excitation in all the mixtures under study were significantly lower as compared to the nanosecond ignition due to the local nature of the energy deposit in the microsecond discharge.

A method for detonation initiation has been developed which allows one to decrease the DDT length in smooth tubes to several tube diameters due to nonequilibrium mixture excitation in a bulk volume. Mechanisms have been proposed claiming that simultaneous mixture ignition in a large number of discharge cells and/or Zeldovich's gradient mechanism may lead to the rapid formation of a detonation wave.

Acknowledgments

This research was partially supported by the European Office of Aerospace Research and Development/Civilian Research and Development Foundation (Project GAP 1349), General Electric Global Research Center (Contract A02), Global Energy Foundation (Grant MG-2006/04/6), National Agency for Science and Innovation (Contract 02.442.11.7335), and the Russian Foundation for Basic Research (Grant 02-03-33376). The research was also supported by an individual grant from the National Agency for Education in the framework of the Program for development of scientific potential of higher education, "The Study of Kinetics of Complex Reactive Systems under Action of High-Voltage Nanosecond Pulses."

References

[1] Bull, D. C., Elsworth, J. E., and Hooper, G., "Initiation of Spherical Detonation in Hydrocarbon/Air Mixtures," *Acta Astronautica*, Vol. 5, No. 11, 1978, pp. 997–1008. doi:10.1016/0094-5765(78)90005-X

[2] Shchelkin, K. I., "Detonation in Gases in Roughened Tubes," *Zhurnal Tekhnicheskoi Fiziki*, Vol. 17, No. 5, 1947, pp. 613–618.

[3] Brown, C. J., and Thomas, G. O., "Experimental Studies of Ignition and Transition to Detonation Induced by the Reflection and Diffraction of Shock Waves," *Shock Waves*, Vol. 10, No. 1, 2000, pp. 23–32. doi:10.1007/s001930050176

[4] Sorin, R., Zitoun, R., and Desbordes, D., "Optimization of the Deflagration to Detonation Transition: Reduction of Length and Time of Transition," *Shock Waves*, Vol. 15, No. 2, 2006, pp. 137–145. doi:10.1007/s00193-006-0007-4

[5] Smirnov, N. N., and Nikitin, V. F., "Effect of Channel Geometry and Mixture Temperature on Detonation-to-Deflagration Transition," *Combustion, Explosion, and Shock Waves*, Vol. 40, No. 2, 2004, pp. 186–199. doi:10.1023/B:CESW.0000020141.67981.5f

[6] Cooper, M., Jackson, S., Austin, J., Wintenberger, E., and Shepherd, J. E., "Direct Experimental Impulse Measurements for Detonations and Deflagrations," *Journal of Propulsion and Power*, Vol. 18, No. 5, 2002, pp. 1033–1041.

[7] Frolov, S. M., "Liquid-Fueled, Air-Breathing Pulse Detonation Engine Demonstrator: Operation Principles and Performance," *Journal of Propulsion and Power*, Vol. 22, No. 6, 2006, pp. 1162–1169. doi:10.2514/1.17968

[8] Lieberman, D. H., Parkin, K. L., and Shepherd, J. E., "Detonation Initiation by a Hot Turbulent Jet for Use in Pulse Detonation Engines," AIAA Paper 2002-2628, 2002.

[9] Higgins, A. J., Pinard, P., Yoshinaka, A. C., and Lee, J. H. S., "Sensitization of Fuel-Air Mixtures for Deflagration to Detonation Transition," *High-Speed Deflagration and Detonation: Fundamentals and Control*, edited by G. Roy, S. Frolov, D. Netzer, and A. Borisov, Elex-KM Publ., Moscow, Russia, 2001, pp. 45–62.

[10] Achasov, O. V., Labuda, S. A., Kondrashov, V. V., Penyazkov, O. G., Pushkin, R. M., Tarasov, A. I., and Shabunya, S. I., "Focusing of Shock Waves on Reflection from Concave Curvilinear Surfaces," *Journal of Engineering Physics and Thermophysics*, Vol. 65, No. 5, 1993, pp. 1073–1077.

[11] Achasov, O. V., and Penyazkov, O. G., "Some Gasdynamic Methods for Control of Detonation Initiation and Propagation," *High-Speed Deflagration and Detonation: Fundamentals and Control*, edited by G. Roy, S. Frolov, D. Netzer, and A. Borisov, Elex-KM Publ., Moscow, Russia, 2001, pp. 31–44.

[12] Semenov, I., Frolov, S., Markov, V., and Utkin, P., "Shock-to-Detonation Transition in Tubes with Shaped Obstacles," *Pulsed and Continuous Detonations*, edited by G. Roy, S. Frolov, and J. Sinibaldi, Torus Press, Moscow, Russia, 2006, pp. 159–169.

[13] Zeldovich, Y. B., Librovich, V. B., Makhviladze, G. M., and Sivashinskii, G. I., "On the Onset of Detonation in a Nonuniformly Heated Gas," *Journal of Applied Mechanics and Technical Physics*, Vol. 11, No. 2, 1970, pp. 264–270.

[14] Khokhlov, A. M., and Oran, E. S., "Numerical Simulation of Detonation Initiation in a Flame Brush: The Role of Hot Spots," *Combustion and Flame*, Vol. 119, No. 4, 1999, pp. 400–416. doi:10.1016/S0010-2180(99)00058-9

[15] Khokhlov, A. M., Oran, E. S., and Thomas, G. O., "Numerical Simulation of Deflagration-to-Detonation Transition: The Role of Shock-Flame Interactions in Turbulent Flames," *Combustion and Flame*, Vol. 117, Nos. 1–2, 1999, pp. 323–339. doi:10.1016/S0010-2180(98)00076-5

[16] Kapila, A. K., Schwendeman, D. W., Quirk, J. J., and Hawa, T., "Mechanisms of Detonation Formation due to a Temperature Gradient," *Combustion Theory and Modeling*, Vol. 6, No. 4, 2002, pp. 553–594. doi:10.1088/1364-7830/6/4/302

[17] Lee, J. H. S., "Initiation of Gaseous Detonation," *Annual Review of Physical Chemistry*, Vol. 28, Oct. 1977, pp. 75–104. doi:10.1146/annurev.pc.28.100177.000451

[18] Frolov, S. M., Basevich, V. Y., Aksenov, V. S., and Polikhov, S. A., "Detonation Initiation by Controlled Triggering of Electric Discharges," *Journal of Propulsion and Power*, Vol. 19, No. 4, 2003, pp. 573–580.

[19] Cathey, C., Wang, F., Tang, T., Kuthi, A., Gundersen, M. A., Sinibaldi, J. O., Brophy, C., Barbour, E., Hanson, R. K., Hoke, J., Schauer, F., Corrigan, J., and Yu, J., "Transient Plasma Ignition for Delay Reduction in Pulse Detonation Engines," AIAA Paper 2007-443, 2007.

[20] Starikovskii, A. Y., "Deflagration-to-Detonation Control by Non-Equilibrium Gas Discharges and Its Applications for Pulsed Detonation Engine," AIAA Paper 2003-4686, 2003.

[21] Zhukov, V. P., and Starikovskii, A. Y., "Effect of a Nanosecond Gas Discharge on Deflagration to Detonation Transition," *Combustion, Explosion, and Shock Waves*, Vol. 42, No. 2, 2006, pp. 195–204. doi:10.1007/s10573-006-0038-2

[22] Zhukov, V. P., Rakitin, A. E., and Starikovskii, A. Y., "Initiation of Detonation by Nanosecond Gas Discharge," AIAA Paper 2006-952, 2006.

[23] Starikovskii, A. Y., Anikin, N. B., Kosarev, I. N., Mintoussov, E. I., Nudnova, M. M., Rakitin, A. E., Roupassov, D. V., Starikovskaia, S. M., Zavialov, I. N., and Zhukov, V. P., "Nanosecond Pulsed Discharges for Plasma Assisted Combustion and Aerodynamics," *Journal of Propulsion and Power* (to be published).

[24] Starikovskii, A. Y., "The Method of Initiation of Ignition, Intensification of Combustion or Reforming of Fuel-Air and Fuel-Oxygen Mixtures," Patent No. PCT/IB 2006/003106, 2006.

[25] Kaneshige, M., and Shepherd, J. E., "Detonation Database," California Institute of Technology, TR fm97-8, GALCIT, 1997.

J. Powers
Associate Editor